



Optics Letters

Self-calibrating and high-sensitivity microwave phase noise analyzer applying an optical frequency comb generator and an optical-hybrid-based I/Q detector

FANGZHENG ZHANG,¹  JINGZHAN SHI,¹  YU ZHANG,² DE BEN,¹ LIJUN SUN,² AND SHILONG PAN^{1,*} 

¹Key Laboratory of Radar Imaging and Microwave Photonics, Ministry of Education, Nanjing University of Aeronautics and Astronautics, Nanjing 210016, China

²Chongqing Optoelectronics Research Institute, Chongqing 400060, China

*Corresponding author: pans@nuaa.edu.cn

Received 20 August 2018; accepted 13 September 2018; posted 14 September 2018 (Doc. ID 342669); published 10 October 2018

Phase noise analyzers (PNAs) are indispensable for evaluating the short-term stability of microwave signals. In this Letter, a high-sensitivity PNA with self-calibration capability is proposed based on an optical frequency comb generator and an optical-hybrid-based I/Q detector. The negative factors that result in inaccurate measurement, including the direct component interference, amplitude noises of the microwave signal under test and the laser, and phase noise of the laser, are all eliminated through digital signal processing. A proof-of-concept experiment is performed. The established PNA can achieve accurate phase noise measurement with a high sensitivity of -146.1 dBc/Hz at 10 kHz, and the self-calibrating property of the PNA is also verified. © 2018 Optical Society of America

OCIS codes: (060.5625) Radio frequency photonics; (070.1170) Analog optical signal processing; (060.2360) Fiber optics links and subsystems.

<https://doi.org/10.1364/OL.43.005029>

Phase noise indicates the short-term frequency stability of a single-frequency signal [1]. In radar, communication, and navigation systems, high-stability microwave signals are highly demanded [2,3], and a high-sensitivity phase noise analyzer (PNA) is indispensable for measuring microwave signals having a low phase noise. Among the various methods for establishing a PNA, the photonic-delay-line-based frequency discriminator method has attracted a lot of attention because it can achieve a high sensitivity and a large measurement frequency range with the help of microwave photonic technologies [4–7]. In this method, to achieve a high phase noise measurement sensitivity, a large time delay is required [8], which, however, will reduce the reliable offset frequency range for phase noise measurement. By applying the two-channel cross-correlation method [9], the phase noise measurement sensitivity can also be

improved, but the measurement is usually time-consuming, and the system has a high cost. In Ref. [10], a cost-effective real-time ultra-high-sensitivity PNA based on an optical frequency comb (OFC) generator is proposed. By processing the selected $\pm n$ th order comb lines, which carry the n -times magnified phase noise of the signal under test (SUT), the measurement sensitivity of the PNA can be significantly improved. However, a potential problem with this system is that the phase-to-voltage conversion coefficient of the mixer is dependent on the input power, which not only converts the amplitude noises of the SUT and the laser source into a part of the measured phase noise but also requires a calibration before each measurement because the SUTs usually have different powers.

In this Letter, we propose and demonstrate a self-calibrating and high-sensitivity PNA based on an OFC generator and an optical-90-degree-hybrid-based I/Q detector. Figure 1(a) shows the schematic diagram of the proposed PNA. The continuous wave (CW) light from a laser diode (LD) is injected into an OFC generator, which is driven by the SUT having a frequency of f_s . According to Ref. [11], the optical field of the obtained signal is

$$E_1(t) \propto \sum_{n=-\infty}^{n=\infty} [A_n(t) e^{j[2\pi(f_c + nf_s)t + \varphi_c(t) + n\varphi_s(t)]}], \quad (1)$$

where f_c and $\varphi_c(t)$ are the frequency and phase noise of the CW light from the LD, respectively. $\varphi_s(t)$ is the phase noise of the SUT. $A_n(t)$ is the amplitude of the $+n$ th order comb line, which is related to the amplitude and amplitude noise of the CW light and the amplitude and amplitude noise of the SUT. Considering the symmetry of the OFC, the amplitude of the $-n$ th order comb line is equal to that of the n th order comb line, that is, $A_{-n}(t) = A_n(t)$.

The output signal from the OFC generator is amplified by an erbium-doped fiber amplifier (EDFA) and then split into two branches by an optical splitter. In the upper branch, a span of single-mode fiber (SMF) is used to introduce a time delay of τ . Then, the $\pm n$ th order comb lines of the delayed signal are

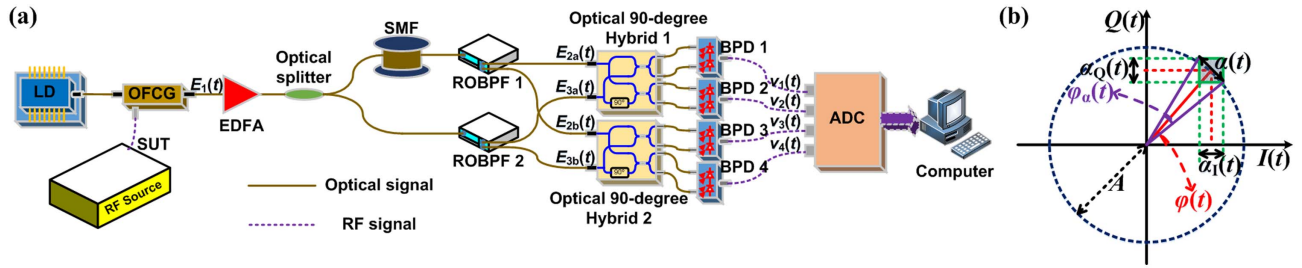


Fig. 1. (a) Schematic diagram of the proposed PNA and (b) diagram for estimating the phase noise floor.

selected out by a dual-output reconfigurable optical bandpass filter (ROBPF). The obtained two optical signals after the ROBPF can be written as

$$\begin{aligned} E_{2a}(t) &\propto A_n(t - \tau) e^{j[2\pi(f_c + nf_s)(t - \tau) + \varphi_c(t - \tau) + n\varphi_s(t - \tau)]}, \\ E_{2b}(t) &\propto A_n(t - \tau) e^{j[2\pi(f_c - nf_s)(t - \tau) + \varphi_c(t - \tau) - n\varphi_s(t - \tau) - \varphi_d]}, \end{aligned} \quad (2)$$

where φ_d is the phase difference between the $+n$ th order and the $-n$ th order comb lines due to the dispersion of the SMF. In the lower branch, the $\pm n$ th order comb lines are filtered out by another ROBPF, and the obtained two optical signals are

$$\begin{aligned} E_{3a}(t) &\propto A_n(t) e^{j[2\pi(f_c + nf_s)t + \varphi_c(t) + n\varphi_s(t)]}, \\ E_{3b}(t) &\propto A_n(t) e^{j[2\pi(f_c - nf_s)t + \varphi_c(t) - n\varphi_s(t)]}. \end{aligned} \quad (3)$$

Next, the two $+n$ th order comb lines from the upper and the lower branches are sent to the two input ports of an optical 90-degree hybrid, respectively [12]. After the hybrid, two balanced photodiodes (BPD1 and BPD2) are followed to implement optical-to-electrical conversion. The output electrical signals of BPD1 and BPD2 are

$$\begin{aligned} v_1(t) &\propto 4R_1 Z_L A_n(t) A_n(t - \tau) \cos(\varphi_1(t) + \varphi_2(t)), \\ v_2(t) &\propto 4R_2 Z_L A_n(t) A_n(t - \tau) \sin(\varphi_1(t) + \varphi_2(t)), \end{aligned} \quad (4)$$

where R_1 and R_2 are the responsivities of BPD1 and BPD2, respectively, Z_L is the input impedance, $\varphi_1(t) = 2\pi f_c \tau + \varphi_c(t) - \varphi_c(t - \tau)$, and $\varphi_2(t) = 2\pi n f_s \tau + n[\varphi_s(t) - \varphi_s(t - \tau)]$. Similarly, the two $-n$ th order comb lines from the upper and the lower branches are sent to another optical 90-degree hybrid, which is followed by another pair of BPDs (BPD3 and BPD4). The obtained two electrical signals are

$$\begin{aligned} v_3(t) &\propto 4R_3 Z_L A_n(t) A_n(t - \tau) \cos(\varphi_d + \varphi_1(t) - \varphi_2(t)), \\ v_4(t) &\propto 4R_4 Z_L A_n(t) A_n(t - \tau) \sin(\varphi_d + \varphi_1(t) - \varphi_2(t)), \end{aligned} \quad (5)$$

where R_3 and R_4 are the responsivities of BPD3 and BPD4, respectively. The obtained four electrical signals in Eqs. (4) and (5) are digitized by a four-channel analog-to-digital converter (ADC), and the obtained digital signals are processed to acquire the phase noise of the SUT.

Based on Eqs. (4) and (5), $\varphi_2(t)$ can be calculated by

$$\varphi_2(t) = \arctan \left[\frac{\frac{R_1}{R_3} v_3(t) - v_1(t)}{\frac{R_1}{R_2} v_2(t) + \frac{R_1}{R_4} v_4(t)} \right] + \frac{\varphi_d}{2}. \quad (6)$$

Considering the variation of $\varphi_1(t)$ due to the phase noise of a typical LD would exceed 2π in a short observation time [13], according to Eqs. (4) and (5), the maximum value of $v_i(t)$ is proportional to R_i , and thus R_1/R_i can be figured out by

$$\frac{R_1}{R_i} = \frac{\max[v_1(t)]}{\max[v_i(t)]}, \quad i = 2, 3, 4. \quad (7)$$

In Eq. (6), φ_d can be treated as a constant, because the phase fluctuation due to the interreaction between the phase noise of a commercial LD and the dispersion of an SMF with a length of several kilometers can be neglected. Thus, the power spectral density (PSD) of $\varphi_2(t)$ at nonzero offset frequencies can be calculated by neglecting the $\varphi_d/2$ term in Eq. (6). Finally, the phase noise of the SUT can be achieved via

$$L(f) = \frac{s_{\varphi_2}(f)}{8n^2 \sin^2(\pi f \tau)}, \quad f > 0, \quad (8)$$

where $s_{\varphi_2}(f)$ is the PSD of $\varphi_2(t)$.

In this method, the estimated phase $\varphi_2(t)$ in Eq. (6) is related to the n -times magnified phase variation of the SUT. Thus a high phase noise measurement sensitivity can be achieved. To show how the measurement sensitivity is affected by n , the phase noise floor of the PNA is analyzed when choosing different n and considering the internal noises of the measurement system. Here, the internal noise sources, including the shot noise, flicker noise, and thermal noise, are mainly from the active devices in the system, such as the BPDs and the ADC [14]. We define the terms $(R_1 v_2(t)/R_2 + R_1 v_4(t)/R_4)$ and $(R_1 v_3(t)/R_3 - v_1(t))$ in Eq. (6) as $I(t)$ and $Q(t)$, respectively. Since the noises in the BPDs and the ADC are uncorrelated, the noise signals in $I(t)$ and $Q(t)$ are also uncorrelated. In Fig. 1(b), $\alpha_I(t)$ and $\alpha_Q(t)$ are the uncorrelated noise signals in $I(t)$ and $Q(t)$, respectively, A is the signal amplitude that is proportional to the power of the selected comb lines, and $\varphi(t)$ equals $\varphi_2(t) - \varphi_d/2$. When $\alpha_I(t)$ and $\alpha_Q(t)$ are far less than A , the phase fluctuation due to the noises is

$$\varphi_\alpha(t) \approx \frac{\sqrt{|\alpha_I(t)|^2 + |\alpha_Q(t)|^2}}{A} = \frac{\alpha(t)}{A}. \quad (9)$$

We define the PSD of $\varphi_\alpha(t)$ as $s_{\varphi_\alpha}(f)$. To achieve accurate phase noise measurement, the PSD of $\varphi_2(t)$, that is, $s_{\varphi_2}(f)$, should satisfy the following condition:

$$s_{\varphi_2}(f) \geq s_{\varphi_\alpha}(f) = \frac{s_\alpha(f)}{A^2}, \quad (10)$$

where $s_\alpha(f)$ is the PSD of $\alpha(t)$. According to Eq. (8), the minimum phase noise that can be accurately measured is

$$L_{\min}(f) = \frac{s_\alpha(f)}{8A^2 n^2 \sin^2(\pi f \tau)}. \quad (11)$$

Equation (11) indicates that, if A is a constant, the phase noise floor will be improved by choosing a larger n , and the phase

noise floor is improved by $20 \lg(n)$ dB compared with the case applying the ± 1 st order comb lines.

In addition to the high measurement sensitivity, the proposed method also has the following advantages. First, thanks to the use of balanced photodetection, the obtained signals in Eqs. (4) and (5) are free from the direct component (dc) interference, which is undesirable in zero-intermediate-frequency signal processing [7]. Besides, in obtaining Eq. (6), the amplitude noises of the SUT and the laser and the phase noise of the laser $\varphi_c(t)$ are all eliminated, which helps to achieve an accurate phase noise measurement. Furthermore, the value of R_1/R_i in Eq. (7) is acquired during the phase noise measurement process applying the same sampled data, which means a self-calibrating operation is achieved.

To verify the feasibility of the proposed PNA, a proof-of-concept experiment is carried out. A continuous-wave light at 1550.52 nm with a power of 19 dBm is generated by an LD (TeraXion, PS-NLL-1550.52-080-000-A1), which has a linewidth of 5 kHz. The light is sent to an OFC generator (Optical Comb, WETC-01-25) that is driven by the SUT. The obtained OFC is amplified by an EDFA (Amonics, AEDFA-35-B-FA) and then split into two branches by an optical splitter. The signal in the upper branch is delayed by a span of SMF with a length of 2 km and a dispersion of 17 ps/(nm·km) at 1550 nm. After the SMF, the $\pm n$ th comb lines are selected out by a ROBPF (Finisar, Waveshaper 16000A). In the lower branch, the $\pm n$ th order comb lines are selected out using two tunable optical filters (Yenista, XTM-50/S). The two $+n$ th order comb lines and the two $-n$ th order comb lines are sent into an optical 90-deg hybrid (Kylia, COH28), respectively. Following the optical hybrids, four BPDs (Thorlabs, PDB450C) are used to implement square-law detection. The analog voltages at the output of the BPDs are converted to digital signals by a four-channel ADC (National Instruments, PCI-4462) with a sampling rate of 204.8 kSa/s. The digitalized data are sent to a computer for calculating the phase noise.

First, phase noise measurement of a 25-GHz signal generated by a commercial microwave signal source (Agilent, E8257D-option 567) is tested with the established PNA. Figure 2(a) shows the optical spectrum of the generated OFC, which consists of more than 40 comb lines. By adjusting the central wavelength and bandwidth of the ROBPFs to make them have filter responses as shown in Figs. 2(b) and 2(c), the ± 10 th order comb lines are selected, of which the spectra are also shown in Figs. 2(b) and 2(c). Figure 3 shows the digitalized signals of $v_1(t)$, $v_2(t)$, $v_3(t)$, and $v_4(t)$ in a period of 0.2 s, where the phase variations of the waveform are larger than 2π in a temporal duration less than 0.15 s, indicating the calculation in Eq. (7) is feasible. Applying these data, the phase noise of the 25-GHz signal can be calculated based on Eqs. (6)–(8). The result is shown in Fig. 4, in which the phase noise measured by a commercial PNA (R&S, FSWP50) is also depicted as a comparison. As can be seen, the curve measured by the proposed PNA agrees well with that measured by the commercial PNA, especially at offset frequencies larger than 1 kHz. The deviation between the two results at an offset frequency below 1 kHz is mainly attributed to the coefficient of $1/8n^2 \sin^2(\pi f \tau)$ in Eq. (8), which is infinite at zero offset frequencies. This is a common problem for all frequency-discriminator-based PNAs. Another factor resulting in the deviation is the optical phase fluctuations thermally induced in the separated paths of the proposed PNA, which is a slow-varying process [15].

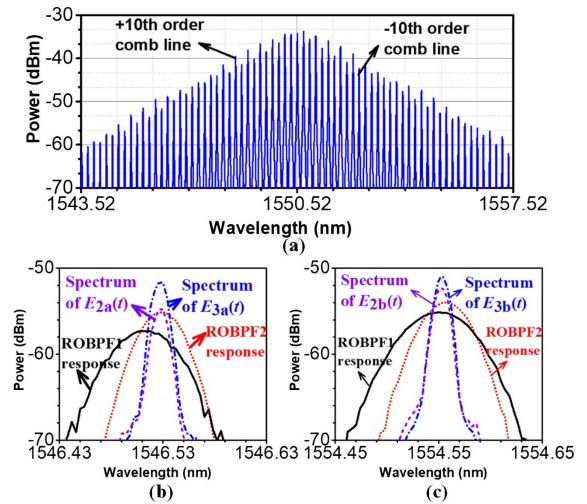


Fig. 2. (a) Optical spectrum of the OFC, (b) responses of the ROBPFs for selecting the +10th order comb lines and the spectra of the selected +10th order comb lines, and (c) responses of the ROBPFs for selecting the -10th order comb lines and the spectra of the selected -10th order comb lines.

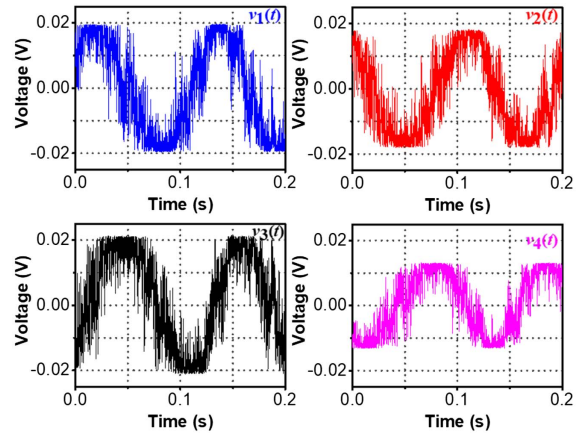


Fig. 3. Digitalized signals of $v_1(t)$, $v_2(t)$, $v_3(t)$, and $v_4(t)$ in a period of 0.2 s.

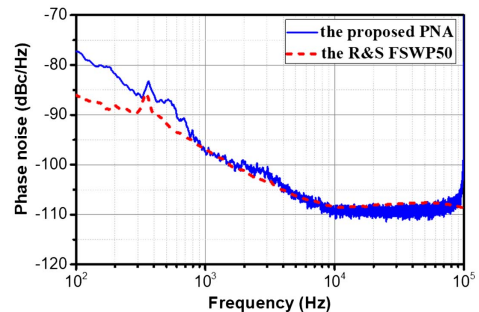


Fig. 4. Phase noise of a 25-GHz signal measured by the proposed PNA and that measured by a commercial PNA.

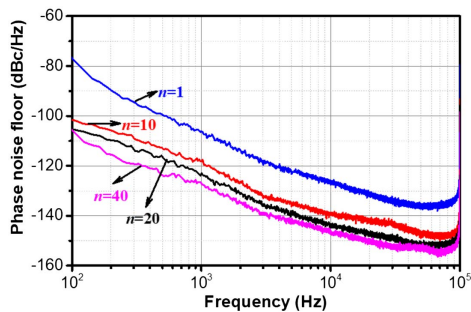


Fig. 5. Phase noise floor of the proposed PNA when n is chosen as 1, 10, 20, and 40, respectively.

Then the phase noise measurement sensitivity is investigated by measuring the phase noise floor of the established PNA, which is implemented according to the method in Ref. [6]. Figure 5(a) shows the measured phase noise floor of the established PNA when n is chosen as 1, 10, 20, and 40, respectively. As can be seen, when selecting the ± 1 st, the ± 10 th, the ± 20 th, and the ± 40 th order comb lines, the phase noise floor at 10 kHz offset frequency is -127.6 , -138.9 , -144.1 , and -146.1 dBc/Hz, respectively. It is found that although the phase noise floor is improved as the increase of n , the improvement shows a deviation from the ideal case as indicated in Eq. (11). This is mainly caused by the fact that, in our experiment, the optical frequency comb line with a higher order has less power, as shown in Fig. 2(a), which means the value of A drops as the increase of n .

It should be noted that, although applying higher order comb lines can help to improve the phase noise measurement sensitivity, another factor must be considered when choosing the proper comb lines. Based on Eq. (6), to estimate the phase $\varphi_2(t)$ without ambiguity, the following condition should be satisfied:

$$k\pi - \frac{\pi}{2} < \varphi_2(t) - \frac{\varphi_d}{2} \leq k\pi + \frac{\pi}{2}, \quad k \in \mathbf{Z}. \quad (12)$$

Choosing a larger n would result in a smaller varying range of $\varphi_s(t) - \varphi_s(t - \tau)$ that can be estimated without ambiguity. Therefore, there is a trade-off between the sensitivity and the maximum phase noise that can be accurately measured. To demonstrate this property, the phase noise of a single-frequency signal generated by a vector network analyzer (R&S, ZVA67) is measured by the established PNA applying the ± 1 st and the ± 10 th order comb lines, respectively. The results are shown in Fig. 6(a), where the phase noise measured by a commercial PNA is also included. As can be seen, when $n = 1$, the measured phase noise agrees well with that measured by the commercial PNA, while, when $n = 10$, an erroneous measurement result is obtained. This can be explained by the calculated phase $\varphi_2(t) - \varphi_d/2$ when n is chosen as 1 and 10, respectively, as shown in Fig. 6(b). When $n = 1$, the estimated phase $\varphi_2(t) - \varphi_d/2$ is accurate since it is kept within the range from $-\pi/2$ to $\pi/2$, while when $n = 10$, phase estimation ambiguity appears because of the phase jumps across $-\pi/2$ or $\pi/2$, and an incorrect phase noise measurement result is obtained.

In conclusion, we have proposed and experimentally demonstrated a microwave PNA applying an OFC generator and an

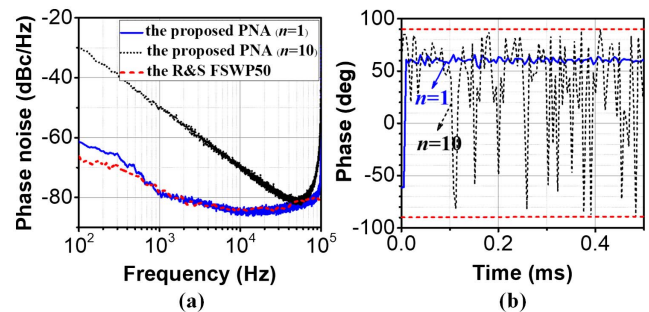


Fig. 6. (a) The phase noise of a signal with poor short-term frequency stability measured by the proposed PNA and that measured by the commercial PNA, and (b) calculated phase term $\varphi_2(t) - \varphi_d/2$ in the cases when the ± 1 st and the ± 10 th comb lines are selected, respectively.

optical 90-deg hybrid. Compared with the work in Ref. [10], the proposed PNA is free from complex calibration and interferences from the amplitude noises of the SUT and the laser. Compared with our previous work using an I/Q mixer for phase noise measurement [7], the proposed PNA is free from additional procedures to deal with the dc component that is undesirable in zero-intermediate-frequency signal processing. In addition, the proposed PNA can achieve a much lower phase noise floor through measuring the multiple phase noise.

Funding. Natural Science Foundation of Jiangsu Province (SBK2018030017); National Natural Science Foundation of China (NSFC) (61527820, 61871214); Postgraduate Research & Practice Innovation Program of Jiangsu Province (KYCX17_0289); Jiangsu Provincial Program for High-Level Talents in Six Areas (DZXX-005); Fundamental Research Funds for the Central Universities (NS2018028).

REFERENCES

1. D. B. Leeson, *IEEE Trans. Ultrason. Ferroelectr. Freq. Control* **63**, 1208 (2016).
2. F. Zhang, Q. Guo, Z. Wang, P. Zhou, G. Zhang, J. Sun, and S. Pan, *Opt. Express* **25**, 16274 (2017).
3. A. G. Armada and M. Calvo, *IEEE Commun. Lett.* **2**, 11 (1998).
4. S. Pan and J. Yao, *J. Lightwave Technol.* **35**, 3498 (2017).
5. F. Zhang, D. Zhu, and S. Pan, *Electron. Lett.* **51**, 1272 (2015).
6. D. Zhu, F. Zhang, P. Zhou, and S. Pan, *Opt. Lett.* **40**, 1326 (2015).
7. F. Zhang, J. Shi, and S. Pan, *Opt. Express* **25**, 22760 (2017).
8. K. Volyanskiy, J. Cussey, H. Tavernier, P. Salzenstein, G. Sauvage, L. Larger, and E. Rubiola, *J. Opt. Soc. Am. B* **25**, 2140 (2008).
9. P. Salzenstein, J. Cussey, H. Tavernier, P. Salzenstein, G. Sauvage, L. Larger, and E. Rubiola, *Acta Phys. Pol. A* **112**, 1107 (2007).
10. N. Kuse and M. E. Fermann, *Sci. Rep.* **7**, 2847 (2017).
11. T. Saitoh, S. Mattory, S. Kinugawa, K. Miyagi, A. Taniguchi, M. Kourogi, and M. Ohtsu, *J. Lightwave Technol.* **16**, 824 (1998).
12. T. R. Clark, S. R. O'Connor, and M. L. Dennis, *IEEE Trans. Microw. Theory Tech.* **58**, 3039 (2010).
13. F. Zhang, Y. Li, J. Wu, W. Li, X. B. Hong, and J. Lin, *IEEE Photon. Technol. Lett.* **24**, 1577 (2012).
14. J. M. Ávila-Ruiz, A. Moscoso-Mártir, E. Durán-Valdeiglesias, L. Moreno-Pozas, J. de-Oliva-Rubio, and I. Molina-Fernández, *J. Electr. Comput. Eng.* **2014**, 1 (2014).
15. T. Musha, J. Kamimura, and M. Nakazawa, *Appl. Opt.* **21**, 694 (1982).